JACS
JOURNAL OF THE AMERICAN CHEMICAL SOCIETY

Subscriber access provided by ISTANBUL TEKNIK UNIV

Article

Molecular Clusters in Two-Dimensional Surface-Confined Nanoporous Molecular Networks: Structure, Rigidity, and Dynamics

Shengbin Lei, Kazukuni Tahara, Xinliang Feng, Shuhei Furukawa, Frans C. De Schryver, Klaus Müllen, Yoshito Tobe, and Steven De Feyter

J. Am. Chem. Soc., **2008**, 130 (22), 7119-7129 • DOI: 10.1021/ja800801e • Publication Date (Web): 09 May 2008

Downloaded from http://pubs.acs.org on February 8, 2009

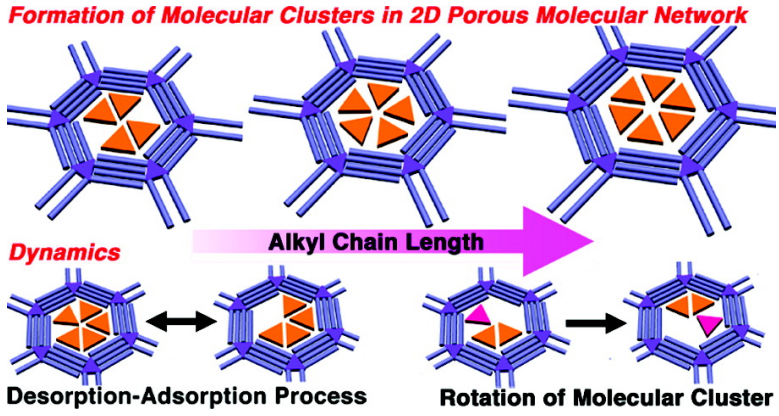

More About This Article

Additional resources and features associated with this article are available within the HTML version:

- Supporting Information
- Links to the 2 articles that cite this article, as of the time of this article download
- Access to high resolution figures
- Links to articles and content related to this article
- Copyright permission to reproduce figures and/or text from this article

View the Full Text HTML

ACS Publications
High quality. High impact.

Journal of the American Chemical Society is published by the American Chemical Society. 1155 Sixteenth Street N.W., Washington, DC 20036

J|A|C|S
ARTICLES

Published on Web 05/09/2008

Molecular Clusters in Two-Dimensional Surface-Confined Nanoporous Molecular Networks: Structure, Rigidity, and Dynamics

Shengbin Lei,† Kazukuni Tahara,‡ Xinliang Feng,§ Shuhei Furukawa,† Frans C. De Schryver,† Klaus Müllen,§ Yoshito Tobe,*,‡ and Steven De Feyter*,†

Department of Chemistry, Division of Molecular and Nanomaterials, Laboratory of Photochemistry and Spectroscopy, and Institute of Nanoscale Physics and Chemistry, Katholieke Universiteit Leuven (KULeuven), Celestijnenlaan 200 F, B-3001 Leuven, Belgium, Division of Frontier Materials Science, Graduate School of Engineering Science, Osaka University, Toyonaka, Osaka 560-8531, Japan, and Max Planck Institute for Polymer Research, Ackermannweg 10, 55128 Mainz, Germany

Received January 31, 2008

Abstract: The self-assembly of a series of hexadehydrotribenzo[12]annulene (DBA) derivatives has been investigated by scanning tunneling microscopy (STM) at the liquid/solid interface in the absence and presence of nanographene guests. In the absence of appropriate guest molecules, DBA derivatives with short alkoxy chains form two-dimensional (2D) porous honeycomb type patterns, whereas those with long alkoxy chains form predominantly dense-packed linear type patterns. Added nanographene molecules adsorb in the pores of the existing 2D porous honeycomb type patterns or, more interestingly, they even convert the guest-free dense-packed linear-type patterns into guest-containing 2D porous honeycomb type patterns. For the DBA derivative with the longest alkoxy chains ($OC_{20}H_{41}$), the pore size, which depends on the length of the alkoxy chains, reaches 5.4 nm. Up to a maximum of six nanographene molecules can be hosted in the same cavity for the DBA derivative with the $OC_{20}H_{41}$ chains. The host matrix changes its structure in order to accommodate the adsorption of the guest clusters. This flexibility arises from the weak intermolecular interactions between interdigitating alkoxy chains holding the honeycomb structure together. Diverse dynamic processes have been observed at the level of the host matrix and the coadsorbed guest molecules.

1. Introduction

Self-assembly of nanometer-sized building blocks into well-defined molecular architectures at surfaces represents one of the important challenges of supramolecular chemistry and material sciences, given the perspective of applications of such systems in the broad area of nanotechnology, e.g. as molecular information storage devices or as functionalized organic surfaces.[1,2] Recently two-dimensional (2D) molecular networks, especially those with void spaces, so-called "2D porous networks", have attracted a lot of interest.[3,4] The host porous networks are typically sustained via hydrogen bonds,[5] metal−ligand coordination bonds,[6] or even van der Waals interactions.[3a,b,7] Such 2D porous networks offer the possibility to immobilize functional units as guest molecules in a repetitive and spatially

* E-mail: tobe@chem.es.osaka-u.ac.jp, Steven.DeFeyter@chem.kuleuven.be
† Katholieke Universiteit Leuven (KULeuven).
‡ Osaka University.
§ Max Planck Institute for Polymer Research.

(1) (a) Barth, J. V.; Costantini, G.; Kern, K. *Nature* **2005**, *437*, 671. (b) Wu, H.; Song, Y.; Du, S.; Liu, H.; Gao, H.; Jiang, L.; Zhu, D. *Adv. Mater.* **2003**, *15*, 1925. (c) Balzani, V.; Credi, A.; Venturi, M. *Nanotoday* **2007**, *2*, 18. (d) Kay, E. R.; Leigh, D. A.; Zerbetto, F. *Angew. Chem., Int. Ed.* **2007**, *46*, 72. (e) Katsonis, N.; Kudernac, T.; Walko, M.; van der Molen, S. J.; van Wees, B. J.; Feringa, B. L. *Adv. Mater.* **2006**, *18*, 1397. (f) Piot, L.; Bonifazi, D.; Samori, P. *Adv. Funct. Mater.* **2007**, *17*, 3689.

(2) (a) De Feyter, S.; De Schryver, F. *Top. Curr. Chem.* **2005**, *258*, 205, and references therein. (b) Hietschold, M.; Lackinger, M.; Griessl, S.; Heckl, W. M.; Gopakumar, T. G.; Flynn, G. W. *Microelectron. Eng.* **2005**, *82*, 207. (c) Chiaravalloti, F.; Gross, L.; Rieder, K. H.; Stojkovic, S. M.; Gourdon, A.; Joachim, C.; Moresco, F. *Nat. Mater.* **2007**, *6*, 30. (d) Gimzewski, J. K.; Joachim, C.; Schlittler, R. R.; Langlais, V.; Tang, H.; Johannsen, I. *Science* **1998**, *281*, 531.

(3) (a) Qiu, X. H.; Wang, C.; Zeng, Q.; Xu, B.; Yin, S.; Wang, H.; Xu, S.; Bai, C. *J. Am. Chem. Soc.* **2000**, *122*, 5550. (b) Liu, Y.; Lei, S.; Yin, S.; Xu, S.; Zheng, Q.; Zeng, Q.; Wang, C. *J. Phys. Chem. B* **2002**, *106*, 12569. (c) Otero, R.; Schöck, M.; Molina, L. M.; Lægsgaard, E.; Stensgaard, I.; Hammer, B.; Besenbacher, F. *Angew. Chem., Int. Ed.* **2005**, *44*, 2270. (d) Dmitriev, A.; Spillmann, H.; Lin, N.; Barth, J. V.; Kern, K. *Angew. Chem., Int. Ed.* **2003**, *42*, 2670. (e) Spillmann, H.; Dmitriev, A.; Lin, N.; Messina, P.; Barth, J. V.; Kern, K. J. *Am. Chem. Soc.* **2003**, *125*, 10725.

(4) (a) Tao, F.; Bernasek, S. L. *J. Am. Chem. Soc.* **2005**, *127*, 12750. (b) Stepanow, S.; Lin, N.; Vidal, F.; Landa, A.; Ruben, M.; Barth, J. V.; Kern, K. *Nano Lett.* **2005**, *5*, 901.

(5) (a) Stöhr, M.; Wahl, M.; Galka, C. H.; Riehm, T.; Jung, T. A.; Gade, L. H. *Angew. Chem., Int. Ed.* **2005**, *44*, 7394. (b) Meier, C.; Ziener, U.; Landfester, K.; Weihrich, P. *J. Phys. Chem. B* **2005**, *109*, 21015. (c) Ruben, M.; Payer, D.; Landa, A.; Comisso, A.; Gattinoni, C.; Lin, N.; Collin, J. P.; Sauvage, J. P.; De Vita, A.; Kern, K. *J. Am. Chem. Soc.* **2006**, *128*, 15644. (d) Perdigão, L. M. A.; Champness, N. R.; Beton, P. H. *Chem. Commun.* **2006**, 538. (e) Zhou, H.; Dang, H.; Yi, J. H.; Nanci, A.; Rochefort, A.; Wuest, J. D. *J. Am. Chem. Soc.* **2007**, *129*, 13774. (f) MacLeod, J. M.; Ivasenko, O.; Perepichka, D. F.; Rosei, F. *Nanotechnology* **2007**, *18*, 424031. (g) Nath, K. G.; Ivasenko, O.; MacLeod, J. M.; Miwa, J. A.; Wuest, J. D.; Nanci, A.; Perepichka, D. F.; Rosei, F. *J. Phys. Chem. C* **2007**, *111*, 16996.

 © 2008 American Chemical Society

Chart 1. Structures of the DBAs **1a**−**f**, nanographene **2** and coronene **3**.

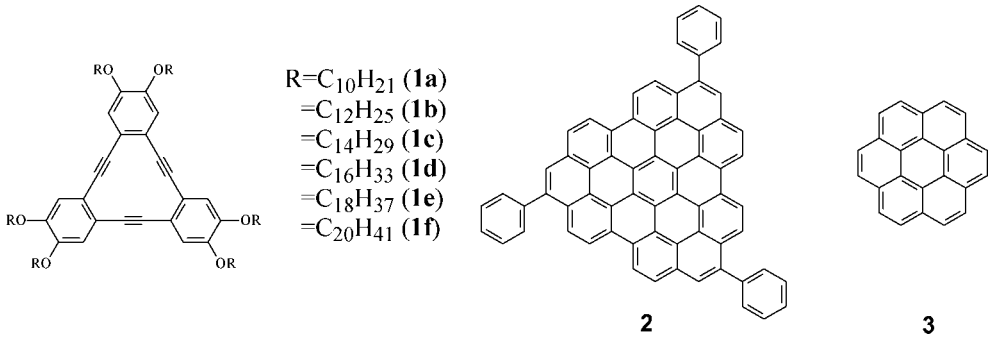

ordered arrangement.[8] The proper choice of the host template layer allows adjustment of not only the intermolecular distance between the guest molecules but also of their relative orientation. Even the physical and dynamic properties, e.g., rotational or switching properties of appropriate guest molecules, can be tuned in response to the environment, which is relevant to the design of molecule-based devices.[9] Typically, cavity sizes ranging from 1 to 5 nm have been reported for single or multicomponent molecular systems.[3–7] Though different kinds of nanoporous structures and 2D host−guest architectures have been reported, the understanding of the mechanism of the formation of nanoporous structures and host−guest interactions on surfaces and interfaces is still in progress.

In surface-confined assemblies of organic molecules, the interplay of adsorbate−adsorbate and adsorbate−substrate interactions is crucial.[1,10] Maximization of these interactions asks for a dense packing, especially when strong directional intermolecular interactions are lacking. Thus, in order to form open porous structures, rigid building blocks capable of forming intermolecular hydrogen bonds or metal coordination bonds are ideal.[5,6] Typically, the resulting porous molecular networks are therefore rigid. Even when relatively strong intermolecular interactions are involved to stabilize the porous networks, other factors play a role too in their formation and stability, such as the solvent at the liquid/solid interface[11,12] or the surface coverage under ultrahigh vacuum conditions.[5a]

Matrix rigidity favors guest selectivity, which is often desired. However, in those cases where the function of the 2D porous matrix is to host a variety of guest molecules, such rigid 2D networks are of limited use. A flexible host network that undergoes slight structural changes to accommodate guest molecules of different size or "aggregation" number would, however, in addition to being able to host a larger set of different guest molecules, provide a reasonably high guest selectivity similar to bioenzymes, such as metalloproteins which recognize their target substrates by an induced-fit mechanism.

Furthermore, to fine-tune the pore size, it seems most appropriate to use straight alkyl chains as spacers, because the length of the alkyl chains can be changed by increments of 1.25 Å (one methylene unit). A potential disadvantage of flexible networks is that they are prone to "collapse" once the network pores become large, which is the result of the tendency toward close packing in order to minimize the total system free energy. However, this flexibility can be turned into an advantage if there is a dramatic structural response to the presence of guest molecules, eventually turning the original nonporous network into a porous network.[13a]

Recently, the formation of nanoporous networks stabilized via van der Waals interactions (via alkyl chain interdigitation) was reported.[13,14] Efficient building blocks are alkylated or alkoxylated dehydrobenzo[12]annulenes (DBA, Chart 1).[13a,14] As discussed above, the size of the cavities in the network can in principle be adjusted by changing the length of the alkoxy substituents. However, due to the tendency of close packing, DBAs with long alkoxy substituents (larger than $OC_{12}H_{23}$) tend to form close-packed linear structures rather than nanoporous honeycomb-type structures. One strategy to favor the formation of nanoporous networks is by tuning the solute concentration.[14c] Another strategy is the addition of a large excess of guest molecules (i.e., coronene), which was shown to induce a structural transformation from linear to nanoporous honeycomb, surface-confined monolayers, in the case of alkoxylated DBAs.[13a] The success of the latter approach was limited, though, to DBAs with alkoxy chain lengths up to $OC_{14}H_{29}$, so that the diameter of the (filled) cavity was still limited (3.9 nm).[13a]

(6) (a) Stepanow, S.; Lingenfelder, M.; Dmitriev, A.; Spillmann, H.; Delvigne, E.; Lin, N.; Deng, X.; Cai, C.; Barth, J. V.; Kern, K. *Nat. Mater.* **2004**, *3*, 229. (b) Lingenfelder, M. A.; Spillmann, H.; Dmitriev, A.; Stepanow, S.; Lin, N.; Barth, J. V.; Kern, K. *Chem. Eur. J.* **2004**, *10*, 1913. (c) Stepanow, S.; Lin, N.; Payer, D.; Schilckum, U.; Klappenberger, F.; Zoppellaro, G.; Ruben, M.; Brune, H.; Barth, J. V.; Kern, K. *Angew. Chem., Int. Ed.* **2007**, *46*, 710.
(7) (a) Spillmann, H.; Kiebele, A.; Stöhr, M.; Jung, T. A.; Bonifazi, D.; Cheng, F.; Diederich, F. *Adv. Mater.* **2006**, *18*, 275. (b) Bonifazi, D.; Kiebele, A.; Stöhr, M.; Cheng, F.; Jung, T.; Diederich, F.; Spillmann, H. *Adv. Funct. Mater.* **2007**, *17*, 1051.
(8) (a) Bonifazi, D.; Spillmann, H.; Kiebele, A.; Wild, M.; Seiler, P.; Cheng, F.; Güntherodt, H. J.; Jung, T.; Diederich, F. *Angew. Chem., Int. Ed.* **2004**, *43*, 4759. (b) Wu, D.; Deng, K.; Zeng, Q.; Wang, C. *J. Phys. Chem. B* **2005**, *109*, 22296. (c) Stepanow, S.; Lin, N.; Barth, J. V.; Kern, K. *Chem. Commun.* **2006**, 2153.
(9) (a) Wintjes, N.; Bonifazi, D.; Cheng, F.; Kiebele, A.; Stöhr, M.; Jung, T.; Spillmann, H.; Diederich, F. *Angew. Chem., Int. Ed.* **2007**, *46*, 4089. (b) Wahl, M.; Stöhr, M.; Spillmann, H.; Jung, T. A.; Gade, L. H. *Chem. Commun.* **2007**, 1349.
(10) De Feyter, S.; De Schryver, F. C. *Chem. Soc. Rev.* **2003**, *32*, 139.
(11) (a) Kampschulte, L.; Lackinger, M.; Maier, A. K.; Kishore, R. S. K.; Griessl, S.; Schmittel, M.; Heckl, W. M. *J. Phys. Chem. B* **2006**, *110*, 10829. (b) Lackinger, M.; Griessl, S.; Heckl, W. M.; Hietschold, M.; Flynn, G. W. *Langmuir* **2005**, *21*, 4984.
(12) (a) Pawin, G.; Wong, K. L.; Kwon, K. Y.; Bartels, L. *Science* **2006**, *313*, 961. (b) Ye, Y.; Sun, W.; Wang, Y.; Shao, X.; Xu, X.; Cheng, F.; Li, J.; Wu, K. *J. Phys. Chem. C* **2007**, *111*, 10138.
(13) (a) Furukawa, S.; Tahara, K.; De Schryver, F. C.; Van der Auweraer, M.; Tobe, Y.; De Feyter, S. *Angew. Chem., Int. Ed.* **2007**, *46*, 2831. (b) Bléger, D.; Kreher, D.; Mathevet, F.; Attias, A. J.; Schull, G.; Huard, A.; Douillard, L.; Fiorini-Debuischert, C.; Charra, F. *Angew. Chem., Int. Ed.* **2007**, *46*, 7404.
(14) (a) Tahara, K.; Furukawa, S.; Uji-i, H.; Uchino, T.; Ichikawa, T.; Zhang, J.; Mamdouh, W.; Sonoda, M.; De Schryver, F. C.; De Feyter, S.; Tobe, Y. *J. Am. Chem. Soc.* **2006**, *128*, 16613. (b) Furukawa, S.; Uji-i, H.; Tahara, K.; Ichikawa, T.; Sonoda, M.; De Schryver, F. C.; Tobe, Y.; De Feyter, S. *J. Am. Chem. Soc.* **2006**, *128*, 3502. (c) Lei, S.; Tahara, K.; De Schryver, F. C.; Van der Auweraer, M.; Tobe, Y.; De Feyter, S. *Angew. Chem., Int. Ed.* **2008**, *47*, 2964.

In this study, we use DBA derivatives **1a−f** with different alkoxy substituents, ranging from decyloxy ($OC_{10}H_{21}$) to icosyloxy ($OC_{20}H_{41}$), to host a large "nanographene" molecule[15] at the liquid/solid interface. We demonstrate that at host concentrations intrinsically favoring the formation of nonporous monolayers, using the second strategy;[16] (1) in the presence of the graphene guest (nanographene **2**), nanoporous honeycomb type structures are formed, even for the largest DBA derivatives with $OC_{20}H_{41}$ chains; (2) filled pores are formed with diameters up to 5.4 nm, which is one of the largest values so far reported;[14c,17] (3) depending on the size of the cavities formed by these DBA derivatives, one to six nanographene **2** guest molecules can be hosted; (4) the host matrix is flexible and responds structurally to the number of nanographene **2** guest molecules adsorbed; and (5) the guest molecules undergo (cooperative) translational and rotational dynamics inside the pores (time scale is on the order of one minute) which can be probed in real time.

2. Experimental Section

The synthesis of the alkoxylated DBAs **1a−f** is described previously.[14]

The DBA derivatives (host) with peripheral alkoxy chains of different length and the nanographene (guest) are first dissolved in 1,2,4-trichlorobenzene (TCB). The concentration of the mother solution of the DBAs is typically 1 g/L. The nanographene solution is saturated (0.034 g/L or 4.1×10^{-5} mol/L as determined by UV−vis spectroscopy).[18] To assemble the host structure, the solution containing a DBA is diluted to 0.05 g/L. For the construction of the host−guest architectures, the original DBA and nanographene solutions are mixed in a 1:1 volume ratio and diluted until 0.05 g/L at the level of the DBAs. For DBAs **1e** and **1f**, the volume ratio of host to guest was adjusted to 1:5 in order to increase the surface coverage of the host−guest architecture.

For STM measurements, a drop of the above solution is applied on a freshly cleaved graphite substrate (HOPG, grade ZYB, Advanced Ceramics Inc., Cleveland, USA). STM images were acquired using a PicoSPM (Agilent) operating in constant current mode with the tip immersed in the solution at room temperature (21−22 °C). Pt/Ir (80/20%) tips were prepared by mechanical cutting. The graphite lattice was recorded by lowering the bias right after obtaining images of the assembly. The drift of the image was corrected using the Scanning Probe Image Processor (SPIP) software (Image Metrology ApS) against the graphite lattice.

3. Results

Self-Assembly of DBA Derivatives: Effect of Alkoxy Chain Length. As reported previously,[13,14] at the TCB/graphite interface DBAs with short alkoxy chains ($\leq OC_{12}H_{25}$) assemble with all six alkoxy chains adsorbed on the surface. The alkoxy chains are fully interdigitated, and well-defined honeycomb nanoporous structures are formed. DBAs with long alkoxy chains ($> OC_{12}H_{25}$) tend to form linear structures with only four alkoxy chains adsorbed. Note, however, that for the DBA concentrations used (0.05 g/L), up until **1d**, honeycomb and close-packed linear structures coexist.[19] In the case of **1e**, honeycomb formation is extremely rare, and for **1f**, no honeycomb formation was observed at all at this concentration. The surface coverage of the honeycomb pattern is more than 95% for **1a** and **1b** (the complete surface is covered by honeycomb patterns except for domain boundaries), 82% for **1c**, 23% for **1d**, and less than 1% for **1e**, confirming a stronger tendency for 2D crystallization into densely packed networks for DBA-derivatives with longer alkoxy chains (Figure 1).[14]

Self-Assembly of Nanographene 2. Unlike the better studied smaller nanographenes such as coronene and hexabenzocoronene, nanographene **2** (to be used as guest in this study) has a 3-fold symmetry, representing a triangular disk with C_3 rather than C_6 symmetry. When self-assembled from TCB on a graphite substrate, it forms a honeycomb rather than a hexagonal structure, in which molecules are adsorbed with their molecular plane parallel to the substrate. The molecules are arranged side-by-side, with one of their corners pointing toward each other forming a void (Figure 2).

Each nanographene appears as a bright triangle with the edge length measured to be about 1.7 nm. This value is smaller than expected from the molecular model, 2.1 nm, taking into account the van der Waals radii. This indicates that only the central π-conjugated part appears bright in the image. The peripheral phenyl groups appear not to contribute significantly to the contrast. This could explain the apparent unexpected large size of the cavities in the honeycomb pattern of nanographene **2**. The unit cell parameters determined after calibration with respect to the graphite lattice are $a = b = 2.4 \pm 0.1$ nm, $\theta = 60° \pm 2$. Note that the triangular geometry of nanographene **2** favors the formation of honeycomb patterns as a result of three edge-to-edge van der Waals interactions per molecule.

Note that nanographene **2** is prochiral and adsorbs to graphite via enantiotopic faces (for details, see Figure S1 in Supporting Information). In order to obtain a closest packing and to optimize the intermolecular interactions, a slight shift between the nanographenes is possible. However, since the three phenyl rings at the periphery are invisible in the STM images, experimentally no evidence of such shift and 2D chirality could be revealed. Thus, in Figure 2, we tentatively suggest an arrangement in which molecules are aligned side-by-side with the same enantiotopic face. Considering the perfect triangular shape of **2**, the energy difference between homochiral and heterochiral domains is expected to be small, so it can not be ruled out that the assembly contains a mixture of both isomers.

Host−Guest Architectures. Recently, we reported the transformation of a linear to honeycomb structure for **1c** ([DBA] = 1 g/L) in response to the addition of appropriate guest molecules, such as coronene.[13a] To complete the transformation, a 7 to 10 times excess of coronene was required. For DBAs with longer alkoxy chains, coronene was not able to induce the transformation. In addition, only planar molecules with large π-conjugated moieties were shown to be able to induce the structural transformation. This transformation was attributed to the gain in free energy upon adsorption of guest molecules, which overcomes the intrinsic instability of a network with large

(15) Feng, X.; Wu, J.; Ai, M.; Pisula, W.; Zhi, L.; Rabe, J. P.; Müllen, K. *Angew. Chem., Int. Ed.* **2007**, *46*, 3033.

(16) Obviously, the host−guest experiments can also be performed at host concentrations which already (nearly) exclusively give rise to nanoporous networks in the absence of guests. The approach followed though allows evaluating the relative performance of different guests in inducing the structural transition studied, or in other words, gives insight in the difference in stability between the guest-host networks.

(17) Schlickum, U.; Decker, R.; Klappenberger, F.; Zoppellaro, G.; Klyatskaya, S.; Ruben, M.; Silanes, I.; Arnau, A.; Kern, K.; Brune, H.; Barth, J. V. *Nano Lett.* **2007**, *7*, 3813.

(18) We often use weight to volume concentration for both the host and guest molecules, since in the surface assembly not only the number of molecules but also the size of the molecules should be taken into account. Molar concentrations are indicated in the figure legends.

(19) The relative surface coverage of the two polymorphs, linear and honeycomb, depends on the concentration of DBAs in the solution.[14c]

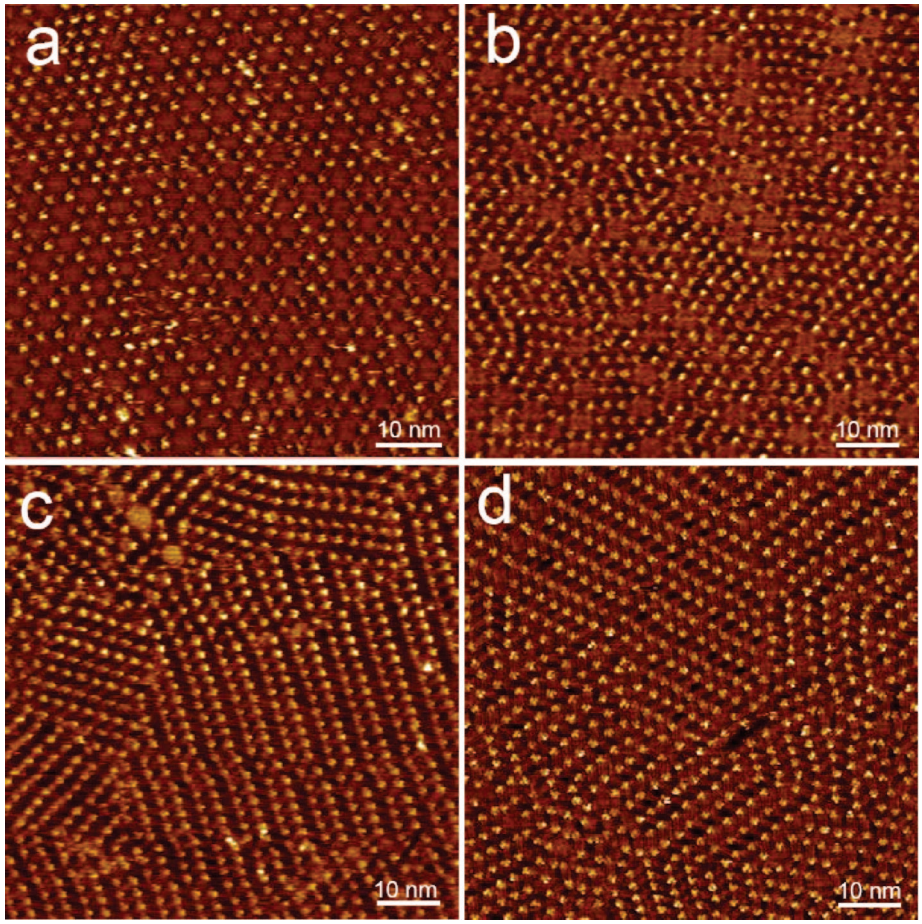

Figure 1. STM images of DBA monolayers at the TCB/graphite interface without guest. (a) **1c**, 3.2×10^{-5} mol/L, $V_{bias} = -0.68$ V, $I_{set} = 305$ pA, (b) **1d**, 2.9×10^{-5} mol/L, $V_{bias} = -0.60$ V, $I_{set} = 490$ pA, (c) **1e**, 2.6×10^{-5} mol/L, $V_{bias} = 0.70$ V, $I_{set} = 49$ pA, (d) **1f**, 2.4×10^{-5} mol/L, $V_{bias} = -1.06$ V, $I_{set} = 266$ pA. Weight to volume concentration of DBAs all equals 0.05 g/L.

"empty" pores. This transition indicates also that the bicomponent host−guest network is more stable than the monocomponent nonporous linear pattern of DBA itself. If this reasoning is correct, we could expect rigid guest molecules that have a stronger adsorption enthalpy, i.e., being larger than coronene, to induce this structural transformation at lower excess concentrations or to induce this transformation too for DBAs with longer alkoxy chains, which intrinsically give rise to larger pores.

The previous study indicated that several coronene molecules are adsorbed in the pores, up to a maximum of seven for **1c**.[13a] Unfortunately, the fast in-plane diffusion of the coronene molecules hindered the exact determination of the number of guest molecules in a pore. Therefore, we anticipate that the use of larger guest molecules, having a stronger interaction with graphite and therefore a lower 2D diffusion constant, will allow visualization of the number of guest molecules adsorbed per pore. In addition, the larger contact area between adjacent nanographenes (edge-to-edge) also has a stabilizing effect.

Figure 3 shows STM images obtained from a mixed solution of **1a** and **2** in TCB. Two different kinds of domains could be revealed in the image, marked as I and II in Figure 3a. Domain I, with brighter contrast, is formed by pure nanographene guest molecules, confirming the strong intermolecular interaction between nanographenes, while domain II is the host−guest architecture formed by coadsorption of **1a** and nanographene **2**. Not all pores are filled with the guest molecules though: some pores appear with low contrast (the empty ones), whereas those containing a guest molecule are bright. Considering the size of the hexagonal pores (2.9 nm corner-to-corner, 2.5 nm edge-to-edge) and nanographene **2** (2.1 nm, the length of one edge), most probably only one nanographene can be trapped. However, due to the incommensurate size, the nanographene is mobile in the void preventing the clear determination of its geometry.[20]

When coadsorbed with **1b**, the basic situation is similar: namely, two kinds of domains are observed, one formed by pure nanographene and the other a honeycomb network formed by coadsorption (Figure 4). However, the increased length of the alkoxy chains induces an increase in the size of the pores (3.5 nm corner-to-corner, 3.0 nm edge-to-edge). The size is nearly commensurate with the size of a nanographene dimer, 3.8 nm in length and 2.1 nm in width (see Figure 2c). High resolution images reveal indeed two different situations: (i) the bright feature inside the cavity is fuzzy and appears with a round shape reflecting a mobile single nanographene, which is trapped in the void and is moving fast compared to the rather slow STM acquisition time (in the order of 170 ms/line) (indicated by the yellow arrow in Figure 4a); (ii) the bright feature has a clearly elongated rhombus-like shape, which we attribute to the formation of a stabilized graphene dimer (indicated by the white arrows in Figure 4a). This is supported by the experimentally observed length (3.3 nm) and width (1.7 nm) of the rhombus-

(20) (a) Heckl, W. M. *Adv. Eng. Mater.* **2004**, *6*, 843. (b) Schull, G.; Douillard, L.; Fiorini-Debuisschert, C.; Charra, F.; Mathevet, F.; Kreher, D.; Attias, A. J. *Nano Lett.* **2006**, *6*, 1360.

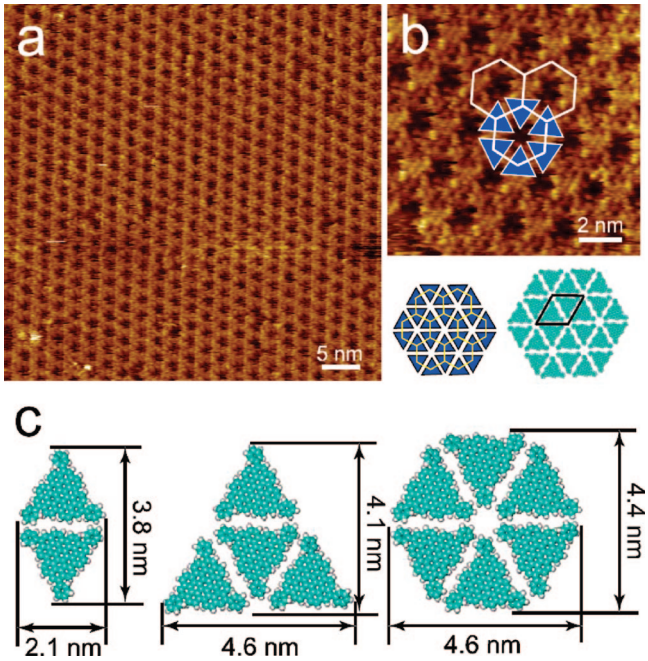

Figure 2. Large-scale (a) and small-scale (b) STM images of a monolayer of nanographene **2** at the TCB/graphite interface (2.1×10^{-6} mol/L). A schematic illustration of the formation of honeycomb structures from triangular building blocks and a tentative molecular model, including the unit cell, is shown below the small-scale STM image. (c) Configuration and dimensions of clusters of nanographene **2**. Tunneling parameters: (a) $V_{bias} = -1.01$ V, $I_{set} = 7$ pA; (b) $V_{bias} = -0.79$ V, and $I_{set} = 86$ pA.

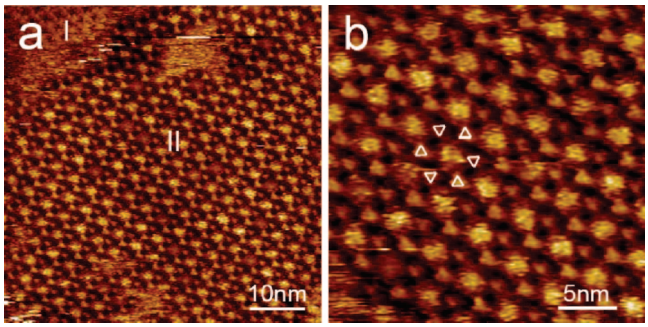

Figure 3. STM images obtained from a mixture of **1a** and nanographene **2** at the TCB/graphite interface. Volume ratio 1:1, concentration: **1a** 4.0×10^{-5} mol/L, nanographene 2.1×10^{-6} mol/L. (a) Two different types of domains are observed: one is the honeycomb host−guest architecture (marked as II), the other one is the 2D crystalline domain formed by the nanographene itself (marked as I). (b) Each DBA aromatic core appears as a small bright triangle, while the guest molecule trapped in the void appears slightly larger and brighter, usually without clear geometry. To guide the eye, a few DBA cores are marked by white triangles in (b). Tunneling parameters: (a) $V_{bias} = 1.04$ V, $I_{set} = 220$ pA; (b) $V_{bias} = 1.04$ V, $I_{set} = 160$ pA.

like feature, which agrees well with a molecular dimer model. Since the actual length of the dimer, 3.8 nm (Figure 2c), is slightly larger than the corner-to-corner distance within the pore (3.5 nm), the host matrix must undergo some kind of relaxation to fit the guest dimer. The long axis of the dimers is always orientated parallel to the edges of the void, pointing to two DBA cores on opposite sides of the honeycomb. This results in three stable orientations of the dimer, corresponding to the 3-fold symmetry of the host matrix (Figure 4b).

For **1c**, STM observations also reveal only honeycomb host−guest architectures and 2D domains of nanographene **2** (Figure 5). This indicates that addition of nanographene **2** is

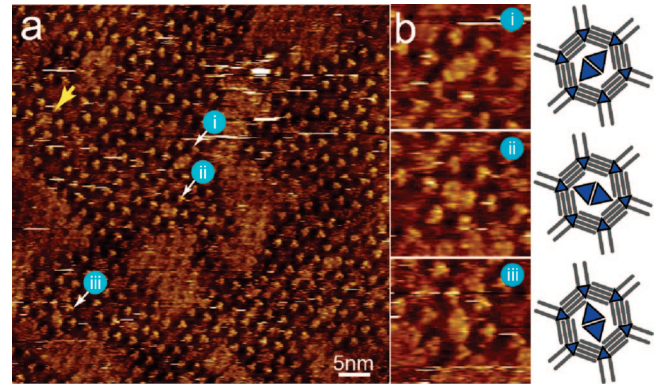

Figure 4. STM images obtained from a mixture of **1b** and nanographene **2** at the TCB/graphite interface. Concentration: **1b** 3.6×10^{-5} mol/L, nanographene **2** 2.1×10^{-6} mol/L. ($V_{bias} = -0.95$ V, $I_{set} = 58$ pA) (a) The three white arrows indicate three nanographene dimers with different orientations. (b) Zooms of these dimers with corresponding schematic models.

indeed efficient to induce the structural transformation from close-packed linear patterns to 2D porous networks of DBAs. Nearly all of the cavities are filled with guest molecules, although the number of guests in each void may differ. This is clearly different from those DBAs with shorter alkoxy chains whose monolayer patterns, in presence of nanographene **2**, are characterized by a large fraction of unoccupied sites. The size of the pores in the network of **1c** is too big for a dimer, but normally not large enough to host more than three guest molecules.

Two types of honeycomb structures could be identified: the normal honeycomb with 3-fold symmetry and distorted honeycombs. In some of these distorted honeycombs (as marked by the white arrow in Figure 5b; see also Figure 5c), the arrangement of the host molecules shows a loss of symmetry. Other less-distorted honeycombs are compressed only in one direction, and the pore still has a 2-fold symmetry (Figure 5d). In the latter kind of honeycombs, the distance between the two DBA cores in the compressed direction decreases from 5.5 to 4.8 nm (indicated in Figure 5b as yellow lines and arrows). In the compressed as well as the normal 3-fold symmetric honeycombs, the number of guest molecules in each cavity could not be accurately determined. However, in some of the distorted honeycombs without symmetry, guest molecules could be identified with submolecular resolution, which is attributed to the strict spatial confinement arising from the distorted host hexagon. For instance, a nanographene hexamer is observed in the distorted honeycomb indicated by the white arrow in Figure 5b. Due to the big size of the hexamer, 4.6 nm in diameter, it cannot fit in a normal honeycomb, and therefore the host matrix is distorted. Note that the observation of a nanographene hexamer is a very rare event, although present in the case of **1c**.

For DBAs with longer alkoxy chains, **1d**, **1e**, and **1f**, in absence of nanographene **2** linear structures are dominant. However, in the presence of nanographene **2**, honeycomb structures are formed nearly exclusively, as shown in Figures 6, 7, and 8 for **1d**, **1e**, and **1f**, respectively. In these cases, the individual guest molecules could be identified clearly. In contrast to the large excess of coronene molecules, which was required to induced the structural transformation (see also Figure S2 in Supporting Information),[13a] a molar ratio (nanographene **2**/DBA) of only 1:20 to 1:2 is sufficient to induce this effect. This

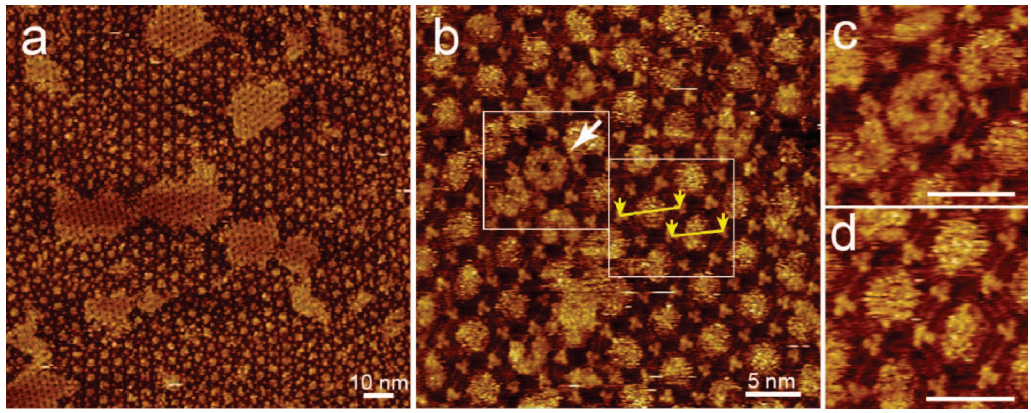

Figure 5. Large scale (a) and high resolution (b) STM images obtained from a mixture of **1c** (3.2×10^{-5} mol/L) and nanographene **2** (2.1×10^{-6} mol/L) at the TCB/graphite interface. (c) and (d) are high-resolution images (not just zooms) of the marked areas in (b). The scale bars correspond to 5 nm. Tunneling parameters: (a) $V_{bias} = -0.57$ V, $I_{set} = 1.0$ nA, (b) (c) and (d) $V_{bias} = -0.60$ V, $I_{set} = 1.0$ nA.

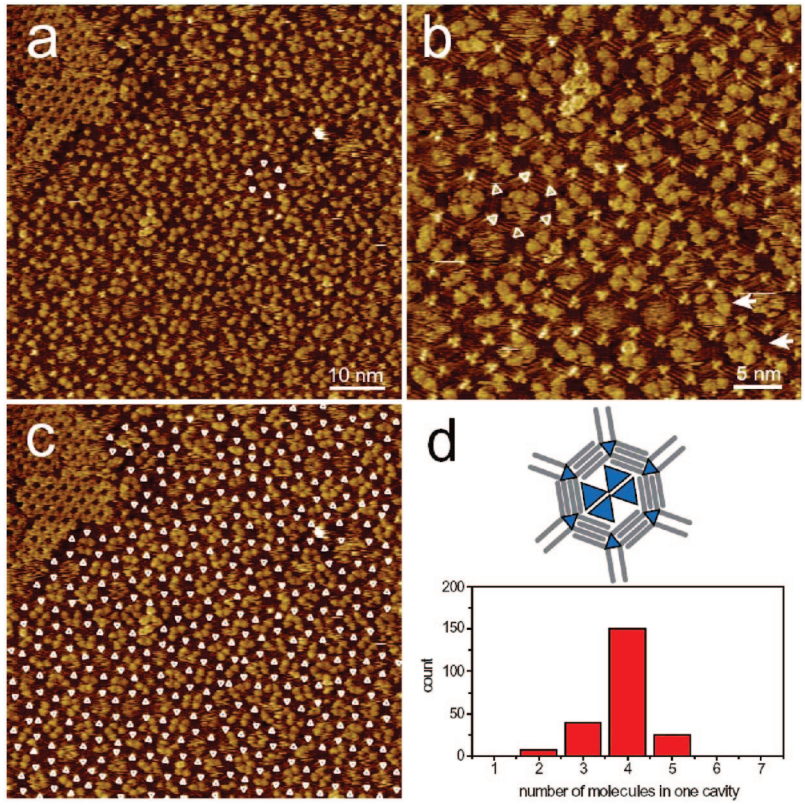

Figure 6. STM images of the host−guest architecture formed by **1d** (2.9×10^{-5} mol/L) in presence of nanographene **2** (2.1×10^{-6} mol/L). Part (a) is identical to (c) in which each DBA core is marked with a triangle to guide the eye. In (b), two pentamers are marked with the white arrows. (d) A schematic model together with a histogram reflecting the distribution of the number of molecules per cavity. Tunneling parameters: (a) and (b) $V_{bias} = -0.79$ V, $I_{set} = 86$ pA.

indicates that nanographene **2** is much more efficient to induce this structural transformation.

Figure 6 shows the host−guest structures formed upon coadsorption of **1d** and nanographene **2**. The DBA cores are marked by bright triangles to guide the eye, so that the guest molecules can be discriminated easily. A large proportion of the honeycombs are distorted (see Figure S3 in Supporting Information for possible distortions of the honeycomb pattern). The number of guest molecules in each void could vary from 2 to 5, depending on the extent of distortion of the host matrix. Another characteristic of this host−guest architecture is that, not only the number but also the orientation of the guest clusters varies from one pore to the other. This makes this architecture quite unique, as it cannot be defined as a 2D crystal, even at the level of the host matrix. Considering the approximate but not perfect hexagonal position of the DBA cores and the disorder of guests and alkyl chains, the overall architecture is more appropriate to be described as a surface confined 2D plastic phase rather than a crystalline phase.

One aspect worth noting is that the arrangement of the molecules in the tetramer observed here is quite different from the configuration illustrated in Figure 2c, in which the triangular nanographene molecules are aligned edge-to-edge, leading to clusters with 3-fold symmetry. In **1d**/nanographene **2** host−guest architectures, no such tetramers have been detected. All experimentally observed tetramers are distorted to fit the cavities.

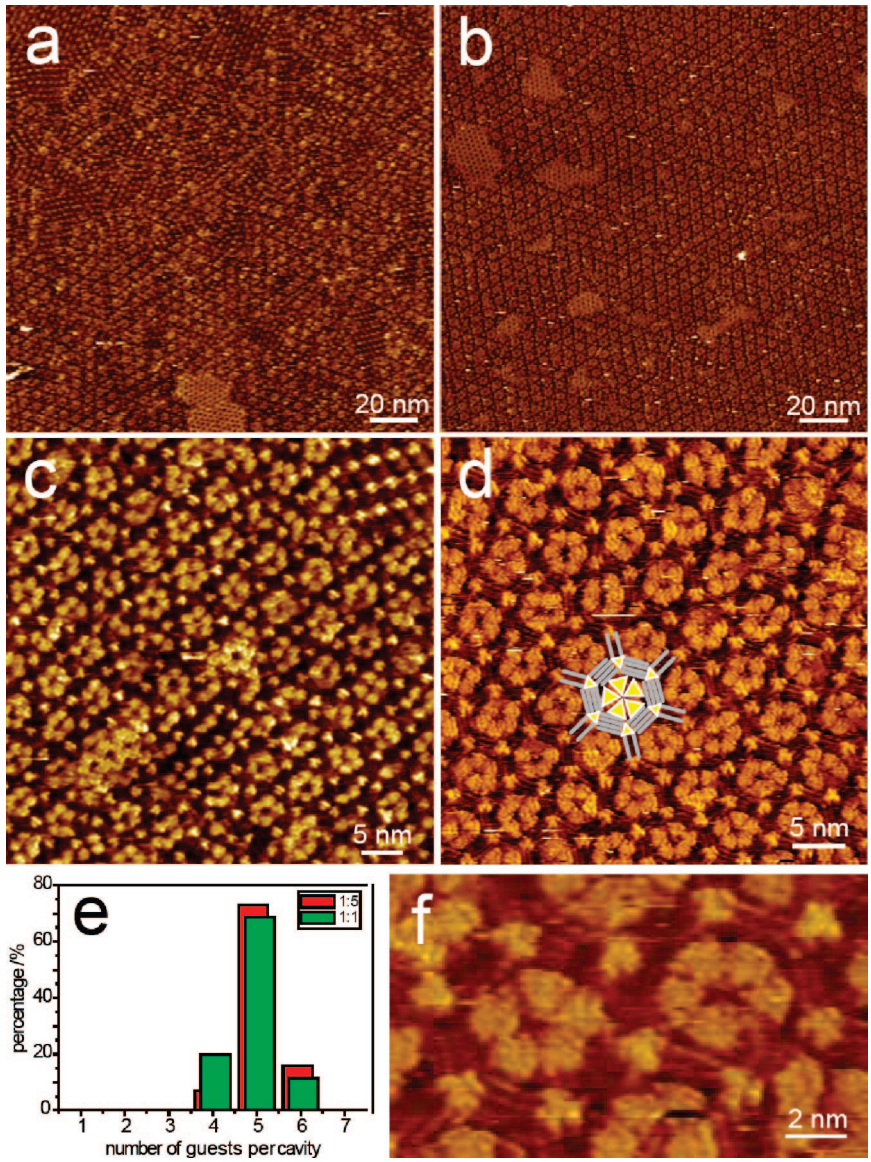

Figure 7. (a) and (b): Large scale images of the host−guest architecture of **1e** and nanographene **2**. The concentration of **1e** is the same (2.6×10^{-5} mol/L) but in (b) the concentration of nanographene **2** (1.1×10^{-5} mol/L) is five times that in (a) (2.1×10^{-6} mol/L). In (a), linear and honeycomb structures coexist on the surface, but in (b), nearly exclusively honeycomb structures are observed. Parts (c) and (d) are the corresponding high resolution images in which the number of guest molecules can be identified. (e) Histogram reflecting the distribution of the number of guest molecules per cavity for both host−guest ratios. (f) Zoom of two differently oriented nanographene pentamers from (d). Tunneling parameters: (a) and (c) $V_{bias} = -0.73$ V, $I_{set} = 73$ pA; (b) and (d) $V_{bias} = -0.95$ V, $I_{set} = 53$ pA.

Also, the guest−host interactions are not ideal. Thus, the stability of the guest molecules in the cavities enabling submolecular imaging must partially be attributed to the spatial confinement of these nanographenes in the hexagonal cavities. It is clear that despite the existence of trimers and pentamers, tetramers are the most abundant species (Figure 6d). Hexamers, which are considered as the most stable clusters have not been detected, which we attribute to the incommensurate size of the voids.

The mere presence of guest molecules is not always sufficient to induce the transition from a nonporous to a porous 2D network, as was shown in the case of coronene, which is only effective for DBA derivatives with alkoxy chains equal or smaller than $OC_{14}H_{29}$ at the host concentration used. The effect of nanographene **2** is definitely stronger (effective for **1a** throughout **1d**), but even though **2** is not able to induce a complete monolayer structure conversion for the longer DBA analogues at a 1:1 volume ratio. In the case of **1e**, mixtures of linear and honeycomb structures are observed to coexist, as shown in Figure 7a. In the high resolution image (Figure 7c) the number and arrangement of the guest molecules in the cavities could be resolved clearly. Most frequently, pentamers are detected (pentamers 70%; hexamers 12%) though their orientation differs from pore to pore.

To explore the influence of the guest-to-host ratio on the monolayer structure transformation as well as on the distribution of the number of guest molecules in each cavity, the relative concentration of the guest was increased 5 times for a given constant concentration of DBA. The results are shown in Figure 7b. It indicates that upon increasing the guest concentration, the honeycomb host−guest architecture becomes the dominant one. No apparent increase of the size or number of nanographene islands was observed. Under these conditions, pentamers are still the most abundant clusters, and the overall distribution of pentamers and hexamers has not changed significantly (pentamer

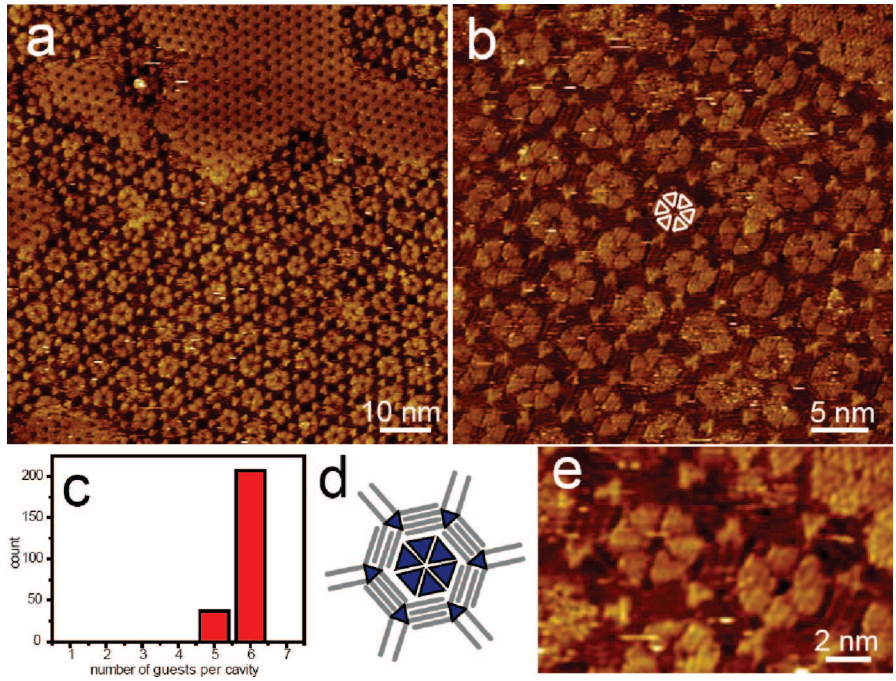

Figure 8. (a) and (b): STM images of host−guest architectures formed by **1f** (2.4×10^{-5} mol/L) and nanographene **2** (1.1×10^{-5} mol/L) ($V_{bias} = -0.71$ V, $I_{set} = 305$ pA). A histogram of the number of molecules per pore is shown in (c), which clearly indicates that the hexamer is dominant. A schematic model and a zoom of two hexamers are shown in (d) and (e), respectively.

73%, hexamer 15%) (Figure 7, parts d and e). This strongly suggests that the number of guest molecules trapped in each cavity is primarily determined by the intrinsic properties, i.e., size and symmetry, of the host honeycombs and the guest molecules, and not by the guest concentration. The guest to host ratio only changes the surface coverage of the honeycomb host−guest architecture.

The self-assembly of **1f** was tested under the same concentration conditions used for **1e** (1:5 volume ratio) (Figure 8, parts a and b). Again, the conversion is complete but nanographene hexamers are now the dominant species (pentamer 15%, hexamer 85%) (Figure 8c). The size of a cavity of **1f** (4.7 nm from edge-to-edge) is practically commensurate with a nanographene hexamer. The orientation of the nanographene molecules in the hexamers is similar, though not identical to the molecular packing in 2D nanographene crystals, and from pore to pore, their orientation is also different (Figures 8, parts b and e): the hexamers are geometrically not perfect, reflecting the symmetry of the host matrix.

4. Discussion

Number of Guest Molecules versus Length of Alkoxy Chains. In most of the reported 2D host−guest structures, a single guest molecule is trapped in each of the cavities, isolating the molecules of interest so to make single molecule studies possible.[20] Forming molecular clusters in the cavity opens the door to control molecular interactions and even chemical reactivity by spatial confinement.[1f] Until now, only very few examples[21] were known of *guest clusters* following the pioneering work of Theobald et al.,[22] reporting on the self-assembly of C_{60} heptamers in the pores of a hydrogen bonded multicomponent network. In the current study, we demonstrate a strategy in which honeycomb nanoporous networks of variable cavity size can be formed by alkyl chain interdigitation. The size of the cavities can be tuned with high precision by varying the length of the alkoxy chains (Table 1). The number of guest molecules trapped in each cavity shows a clear and exclusive dependence on the size of the cavity.

In contrast to nanoporous networks based upon rigid building blocks, the DBA host matrix shows remarkable flexibility: the size, shape, and symmetry of the pores changes in response to the inclusion of guest molecules. The number of guest molecules per cavity always shows a distribution, and honeycombs are often distorted. Such adjustment of the host matrix in response to the inclusion of guest molecules has also been observed in other flexible host networks.[21b,23] For networks based on rigid building blocks, no such phenomenon is observed.

Dynamics within the Host−Guest Matrix. STM has already proven its value for the investigation of structure and dynamics on surfaces and interfaces for both inorganic and organic monolayers.[20,24] For the current system, the liquid/solid interface provides a suitable environment for diverse dynamical processes. The dynamics observed here can be divided into three different categories: in-plane and out-plane dynamics of the host molecule, migration of guest molecules between cavities, and the dynamics of guest molecules inside the cavity.

A. Dynamics of Host Molecules. As mentioned previously, the flexible host matrix undergoes structural changes to adopt

(21) (a) Theobald, J. A.; Oxtoby, N. S.; Champness, N. R.; Beton, P. H.; Dennis, T. J. S. *Langmuir* **2005**, *21*, 2038. (b) Kong, X. H.; Deng; Yang, Y. L.; Zeng, Q. D.; Wang, C. *J. Phys. Chem. C* **2007**, *111*, 9235.

(22) Theobald, J. A.; Oxtoby, N. S.; Phillips, M. A.; Champness, N. R.; Beton, P. H. *Nature* **2003**, *424*, 1029.

(23) Lu, J.; Lei, S. B.; Zeng, Q. D.; Kang, S. Z.; Wang, C.; Wan, L. J.; Bai, C. L. *J. Phys. Chem. B* **2004**, *108*, 5161.

(24) (a) De Feyter, S.; De Schryver, F. C. *J. Phys. Chem. B* **2005**, *109*, 4290. (b) Giancarlo, L. C.; Flynn, G. W. *Acc. Chem. Res.* **2000**, *33*, 491. (c) Miwa, J. A.; Weigelt, S.; Gersen, H.; Besenbacher, F.; Rosei, F.; Linderoth, T. R. *J. Am. Chem. Soc.* **2006**, *128*, 3164. (d) Schunack, M.; Linderoth, T. R.; Rosei, F.; Lægsgaard, E.; Stensgaard, I; Besenbacher, F. *Phys. Rev. Lett.* **2002**, *88*, 156102.

Table 1. Parameters of the Honeycomb Structure Formed by DBAs with Different Alkoxy Substituents **1a**−**f**

	1a	**1b**	**1c**	**1d**	**1e**	**1f**
Repeating period (honeycomb)/nm*	4.1	4.6	5.0	5.5	5.9	6.3
Size of the pore/nm						
Corner-to-corner	2.9	3.5	3.9	4.5	5.0	5.4
Edge-to-edge	2.5	3.0	3.4	3.9	4.3	4.7
Area of unit cell /nm^2	14.6	17.9	21.7	25.7	30.1	34.4
pore area /nm^2	5.4	7.5	10.0	12.8	16.0	19.1
pore fraction /%	37	42	46	50	53	56
Surface coverage of honeycomb (in absence of guests)**	>95%	>95%	89%	23%	<1%	<1%

* Please note that due to the disorder of the host-guest architecture, no accurate unit cell parameters could be determined, thus these values reflect a perfect honeycomb arrangement. ** Weight to volume concentration of DBAs are 0.05 g/L. Molar concentration: **1a**, 4.0×10^{-5} mol/L; **1b**, 3.6×10^{-5} mol/L; **1c**, 3.2×10^{-5} mol/L; **1d**, 2.9×10^{-5} mol/L; **1e**, 2.6×10^{-5} mol/L; **1f**, 2.4×10^{-5} mol/L.

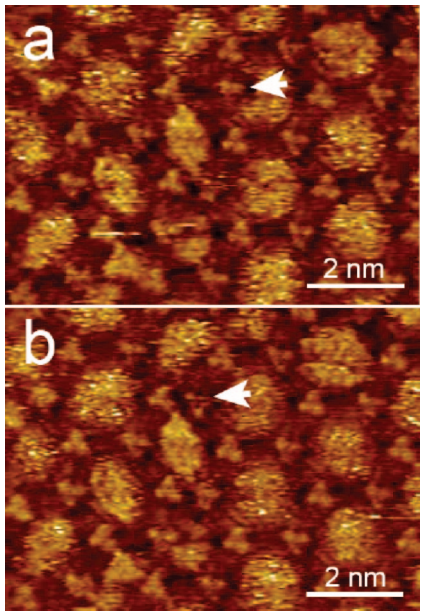

Figure 9. Dynamic processes observed at the liquid/solid interface in the host−guest architecture of **1c**/nanographene **2** ($V_{bias} = -0.60$ V, $I_{set} = 1.0$ nA). The white arrows mark out a host molecule that changes its position during the imaging process. The time interval between these two images is 63 s.

guest molecules during the formation of the host−guest network. Even after completing the host−guest matrix, some structural adjustments could still be observed at specific sites. Figure 9, parts a and b, shows such an event. To the lower left of the host molecule, marked by the white arrow in Figure 9a, a guest dimer is formed in a compressed cavity. This host molecule migrates along the direction shown by the arrow to optimize the interactions with adjacent host and guest molecules. This migration also restores the symmetry of the honeycomb structure to the upper right of this molecule. Thus, the driving force of such dynamic process is considered to be the optimization of the host−guest and host−host interactions.

B. Migration of Guest Molecules between Cavities. Hopping or diffusion of guest molecules between neighboring cavities is the focus of most of the dynamic studies on host−guest systems.[20,25,26b] For DBAs with short alkoxy chains, **1a** and **1b**, a big fraction of cavities are empty and hopping of guest molecules between cavities is frequently observed (see Figure S4 in Supporting Information), though part of those apparent diffusional phenomena might be the result of desorption−readsorption processes. Returning to the discussion on the host−guest architecture of **1d**, in Figure 10, two such events of changing numbers of guest molecules in one cavity were recorded. In the two cavities marked by the white arrows (Figure 10, parts a−d), one guest molecule of the pentamer diffused away or desorbed from the cavity, leaving a tetramer inside. The difference between these two individual events is that in the cavity in the upper part of the image, the configuration of the remaining guest molecules changed after diffusion/desorption of one molecule, whereas in the lower part, the configuration of the guest molecules remained intact.

C. Dynamics of Guest Molecules inside the Cavity. In many of the reported host−guest systems, only a single guest molecule is trapped in each cavity of the host matrix. These trapped guest

(25) (a) Griessl, S. J. H.; Lackinger, M.; Jamitzky, F.; Markert, T.; Hietschold, M.; Heckl, W. M. *Langmuir* **2004**, *20*, 9403. (b) Griessl, S. J. H.; Lackinger, M.; Jamitzky, F.; Markert, T.; Hietschold, M.; Heckl, W. M. *J. Phys. Chem. B* **2004**, *108*, 11556.

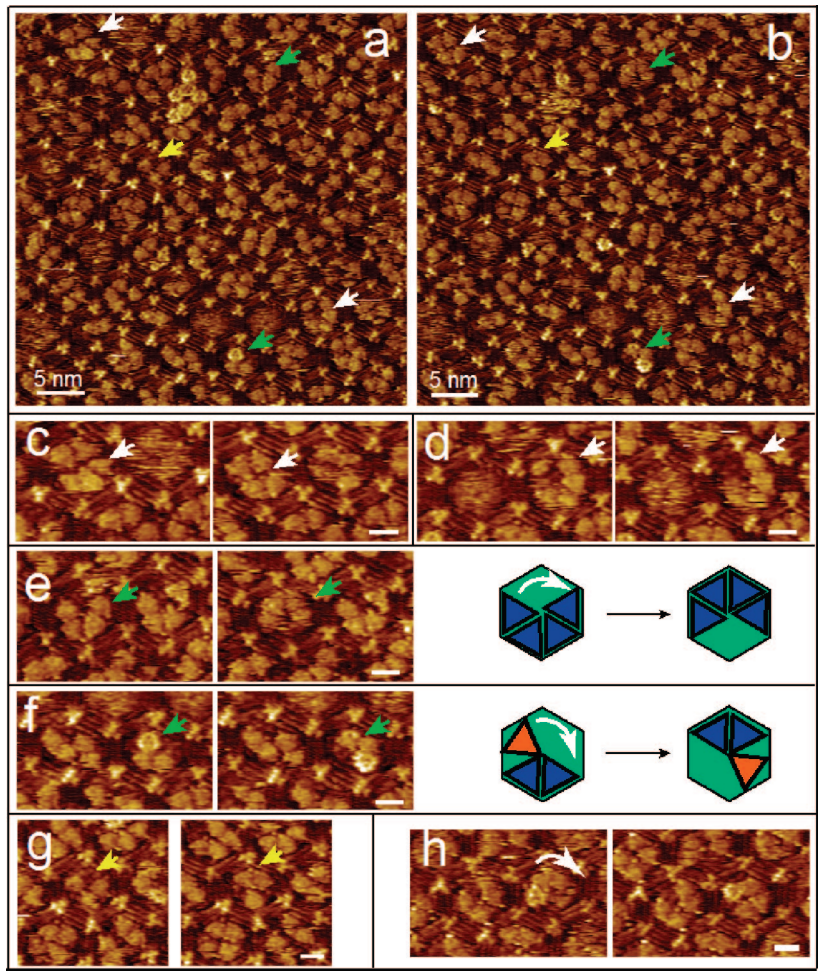

Figure 10. Dynamic processes observed within host−guest architectures of **1d** and nanographene **2** ($V_{bias} = -0.79$ V, $I_{set} = 86$ pA,). The large scale images ((a) and (b)) were obtained consecutively in a time interval of 105 s, zooms below highlight the respective processes; (c) and (d): two individual events of changes in the number of guest molecules as marked by the white arrows in top and bottom of (a) and (b); (e) and (f): two individual rotation events of the guest cluster marked by the green arrows in (a) and (b); and (g): lateral migration of guest molecules inside a cavity (marked by the yellow arrows in (a) and (b)). The drawings in (e) and (f) illustrate the rotation of the corresponding guest clusters in the images. The orange triangle corresponds to the bright triangle in the images: it is an extra nanographene molecule sitting on top of a molecule in the trimer. Another rotation event (not included in (a) and (b)) in which the guest cluster is rotated by 60° is shown in (h). The scale bars correspond to 2 nm.

molecules are either well fixed, allowing for submolecular resolution imaging, or fast rotating, leading to a state in which no stable orientation can be identified.[26] In the current system, for the DBAs with long alkoxy chains, molecular clusters with different numbers of molecules show up in the cavities, and different kinds of dynamic processes could be identified. Translational and rotational motion events of guest molecules are recorded, often regularly. The yellow arrows in Figure 10, parts a and b, indicate a typical translational motion of guest molecules (see also Figure 10g for a zoom). Two of the three guest molecules trapped in that cavity diffuse laterally to form a dimer, while the host matrix remains intact. Such motions are common, especially for guest molecules in the matrices of **1d**, **1e**, and **1f**. Another interesting kind of dynamics is the rotation of guest clusters. The green arrows in Figure 10, parts a and b, mark clusters, which reorient between consecutive images (see also Figure 10, parts e and f, for a zoom). A remarkable feature of this rotation is that the cluster rotates as an entity. Typically, the rotation angles are multiples of 60°. The DBA cores in the host matrix are observed to change their

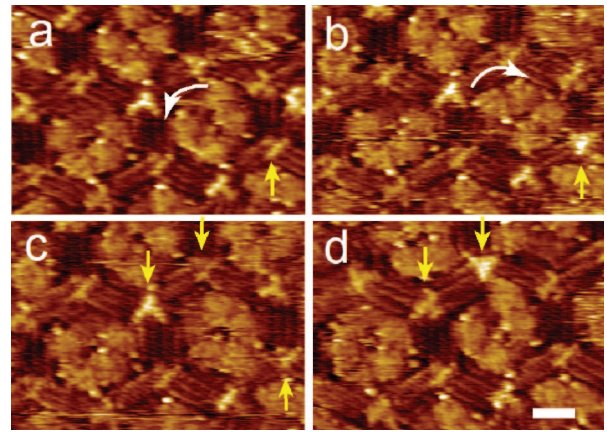

Figure 11. Rotational oscillation of a guest cluster in **1d** cavities ($V_{bias} = -0.79$ V, $I_{set} = 150$ pA). The small yellow arrows indicate those DBA cores changing their contrast upon rotation of the guest cluster. The scale bar corresponds to 2 nm. The time intervals are 63 (a to b), 63 (b to c), and 126 (c to d) s, respectively.

(26) (a) Stöhr, M.; Wahl, M.; Spillmann, H.; Gade, L. H.; Jung, T. A. *Small* **2007**, *3*, 1336. (b) Schull, G.; Douillard, L.; Fiorini-Debuisschert, C.; Charra, F.; Mathevet, F.; Kreher, D.; Attias, A. J. *Adv. Mater.* **2006**, *18*, 2954.

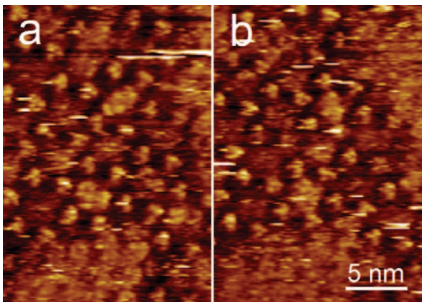

Figure 12. Rotation of nanographene dimers in a **1b** matrix ($V_{bias} = -0.95$ V, $I_{set} = 58$ pA). The time interval between these two consecutive images is 63 s.

contrast during the rotation of the guest cluster (Figure 11). Since the contrast of adsorbed molecules in the STM images is often substrate site dependent,[27] the change in contrast is an indication that the DBA core changes its adsorption site. This is direct evidence that the dynamics of guest clusters is a cooperative motion.

The **1b**/nanographene **2** system represents a special case. Nanographene dimers are formed in the **1b** cavities. Due to the size of the cavity, the dimer can only be oriented with its long axis parallel to the line linking opposite DBA cores. This results in three possible orientations of the dimer. Apparent rotations of the dimer between these three possible orientations are frequently observed (Figure 12).

5. Conclusions

In summary, DBAs with alkoxy substituents form nanoporous networks through interdigitation of the alkyl chains and are capable of acting as hosts to template the assembly of guest molecules. By adjusting the length of the alkoxy substituents, the size of the hexagon cavities can be tuned. However, upon increasing the length of the alkoxy chains, the honeycomb structures collapse and form a dense linear lamella-type structure. Upon addition of large nanographenes as guest molecules, honeycomb DBA networks with alkoxy chains reaching $OC_{20}H_{41}$ are stabilized, resulting in a large repeating period of 6.3 nm and cavities reaching 5.4 nm in diameter. The number of guest molecules in each cavity is exclusively related to the size of the cavity. Up to six nanographene molecules can be hosted in the same cavity for the DBA derivative with the longest alkoxy chains. The structure of the nanographene tetramers and pentamers hosted in the matrix is quite unique and is not observed upon assembly of the nanographene itself.

An important aspect of these host networks is their flexibility. The host matrix changes its structure in order to accommodate the adsorption of the guest clusters. This flexibility arises from the fact that the intermolecular interactions holding the honeycomb structure together are based on weak van der Waals interactions between interdigitating alkyl chains, giving rise to lubricating properties at the molecular level. The alkoxy chains can translate along each other in response to stress imposed by the coadsorption of the guest molecules.

Diverse dynamic processes have been observed. The fact that guest clusters can take up well-defined rotational positions in a cavity is of special interest as it relates to data storage schemes. The ability to adsorb molecular clusters inside the cavities paves the way to use such nanoporous host matrices as nanoreactors for the oligomerization of appropriate guest molecules, for example.

Acknowledgment. This work is supported by K. U. Leuven, the Fund of Scientific Research−Flanders (FWO), the Belgian Federal Science Policy Office through IAP-6/27, a Grant-in-Aid for Scientific Research from the Ministry of Education, Culture, Sports, Science, and Technology, Japan and by the German Science Foundation (FFB/TRR 49).

Supporting Information Available: STM images of assembly of **1e** and **1f** with coronene. This material is available free of charge via the Internet at http://pubs.acs.org.

(27) Sautet, P. *Chem. Rev.* **1997**, *97*, 1097.

JA800801E